ISSN 1028-334X, Doklady Earth Sciences, 2006, Vol. 406, No. 1, pp. 122–127. © Pleiades Publishing, Inc., 2006.
Original Russian Text © N.I. Bezmen, P.N. Gorbachev, A.I. Shalynin, 2006, published in Doklady Akademii Nauk, 2006, Vol. 406, No. 4, pp. 500–506.

GEOCHEMISTRY

Platinum Solubility in Water-Bearing Magnesian Basaltic Melts at 1200°C and 2 kbar

N. I. Bezmen[1], P. N. Gorbachev[1], and A. I. Shalynin[2]

Presented by Academician A.A. Marakushev May 25, 2005

Received June 2, 2005

DOI: 10.1134/S1028334X06010302

The study of the chemical behavior of highly siderophile elements, including platinum group metals (PGM), is of great theoretical and practical significance for understanding the early differentiation of the Earth, mantle and core formation, and the conditions of PGM formation in mafic–ultramafic magmatic complexes. The experimental study of PGM solubility in silicate melts under different physicochemical conditions, together with geochemical investigation, plays an important role in the solution of this problem. Increasingly greater attention has recently been focused on the role of fluids in these processes. With a few exceptions [1, 2], PGM solubility has mainly been studied in the "dry" water-free silicate melts under atmospheric conditions [3, 4]. Therefore, we studied Pt solubility in the water-saturated haplobasaltic melt under high water pressure within a wide oxygen fugacity range spanning the whole interval of the natural magmatic process.

Pd solubility was studied in a melt of $Di_{55}An_{35}Ab_{10}$ (DAA) composition close to diopside–plagioclase eutectics, a magnesian analogue of basaltic magmas, at 1200°C, a fluid pressure of 2 kbar, and f_{O_2} from the HM to WI buffer. The hydrogen mole fraction varied from 0.05 to 0.50, and $\log f_{O_2}$ varied from –2.6 to –11.8. Experiments were conducted in a high gas pressure apparatus using a hydrogen reactor at the Institute of Experimental Mineralogy. The oxygen fugacity was controlled by the double capsule buffer technique under oxidizing conditions (HM–NNO buffers) and by an Ar–H_2 gas mixture that was introduced into the hydrogen reactor of the high-gas-pressure apparatus under reducing conditions ($X_{H_2} > 0.05$) [5]. Temperature was measured by $Pt_{30}Rh/Pt_6Rh$ thermocouples with an accuracy of ±7°C, and pressure was controlled using a Bourdon gauge with an accuracy of ± 50 bar. Samples were quenched by switching off the power with a rate of 130°C/min at 1200–800°C.

Charges were prepared from SiO_2, MgO, CaO, Al_2O_3, and $NaAlO_2$ of reagent and high purity grade. The starting powdered glass was placed in a platinum ampule, diluted with distilled water or 15% H_2O_2 under oxidizing conditions (HM buffer), sealed, and placed into the ultrahigh-gas-pressure apparatus.

After the experiment, glasses (quenched melts) were represented by transparent cylinders 6 mm across and 5–6 mm high. To prevent glass pollution by Pt from the ampule, the outer layers (0.1–0.5 mm) were removed by means of polishing with diamond powder and then boiled for 1 h in concentrated HCl.

Samples were analyzed by the INAA method at Toronto University, Canada, with an accuracy of ±5 rel % using the technique described in [6]. The composition of the fluid was calculated assuming that fluids under the experimental temperature and pressure (1200°C and 2 kbar) behave as ideal gas mixtures.

Experiments of different durations performed to determine the time required for equilibrium showed that the Pt content remained constant in experiments longer than 32 h. Our experiments lasted for 72 h. Duplicate experiments were performed to control the result agreement. One sample was analyzed, while a second sample was used as the starting sample in the experiment at the same conditions.

The fugacities of fluid components and Pt solubility in the silicate melt are listed in Tables 1 and 2. Variations in Pt solubility versus the fugacity of oxygen, water, and hydrogen are shown in Figs. 1 and 2. The aforementioned data indicate that Pt solubility reached 10*n* ppm and varied depending on hydrogen mole fraction and the fugacity of oxygen and water in fluid.

The dependence of the logarithm of solubility C_{Pt} on $\log f_{O_2}$ and other components shows an extremal

[1] *Institute of Experimental Mineralogy, Russian Academy of Sciences, Chernogolovka, Moscow oblast, 142432 Russia; e-mail: bezmen@iem.ac.ru*

[2] *Institute of Solid State Physics, Russian Academy of Sciences, Chernogolovka, Moscow oblast, 142432 Russia*

Table 1. Conditions and results of experiments on Pt solubility in the water-saturated haplobasaltic melt at $T = 1200°C$ and $P = 2$ kbar

Sample no.	Buffer	X_{H_2}	$-\lg f_{O_2}$	f_{H_2O}, bar	Pt, ppm
Pt-83*	HM	$2.12 \cdot 10^{-5}$	2.58	2039	76.200
Pt-84*	HM	$2.12 \cdot 10^{-5}$	2.58	2039	74.988
Pt-110	MnMnO	0.002	6.53	2036	30.720
Pt-142	NNO	0.007	7.67	2025	26.690
Pt-118	–	0.05	9.30	1938	20.610
Pt-153	–	0.05	9.30	1938	21.950
Pt-73	–	0.1	10.02	1836	24.617
Pt-151	–	0.1	10.02	1836	23.400
Pt-72/1*	–	0.2	10.72	1632	30.792
Pt-72/2*	–	0.2	10.72	1632	30.067
Pt-80	–	0.35	11.39	1325	48.610
Pt-74	–	0.50	11.86	1019	54.781

* Duplicate experiments.

Table 2. Pt solubility in the water-saturated DAA melts at $T = 1200°C$ and $P = 2$ kbar.
Parameters of the equation of linear regression $y = kX + A$ of the dependence of $\log C_{Pt}$ on $\log f_{O_2}$, $\log f_{H_2O}$ and $\log f_{H_2}$ for different thermodynamic models (Eqs. (1)–(3)) of Pt solubility

Thermodynamic equation	$k \pm s$	A	R	m
1. Pt (metal) + $\frac{m}{4}O_2 = PtO_{m/2}$ (Melt)				
ox	-0.086 ± 0.033	2.09	0.99	1/3
red	0.172 ± 0.047	–0.32	0.92	2/3
2. Pt (metal) + $\frac{m}{4}O_2 + \frac{m}{2}H_2O = Pt(OH)_{m/2}$ (Melt)				
ox	-0.172 ± 0.034	1.52	0.99	1/3
red	0.285 ± 0.041	0.90	0.94	2/3
3. Pt (metal) + $\frac{m}{2}H_2 = PtH_{m/2}$ (Melt)				
ox	0.164 ± 0.033	1.65	0.99	1/3
red	-0.364 ± 0.074	0.53	0.81	2/3

Note: (m) Effective valence, (R) correlation coefficient, (ox, red) oxidizing and reducing conditions, respectively. In the linear regression equation: $y = \log C_{Pt}$, $X = -\log f_{O_2}$ (for Eq. (1)), $X = -[\frac{1}{2}\log f_{O_2} + \log f_{H_2O}]$ (for Eq. (2)), $X = -\log f_{H_2}$ (for Eq. (3)).

character. In the "oxidizing" range ($\log f_{O_2}$ from HM to MW buffers), Pt solubility shows a positive correlation with f_{O_2}. In the $\log C_{Pt} - \log f_{O_2}$ diagram, the solubility curve shows inflection at $\log f_{O_2} < -9.3$ and hydrogen mole fraction $X_{H_2} \le 0.1$ (wustite stability field) and then a negative correlation with f_{O_2} at f_{O_2} from MW to WI buffers.

As follows from the solubility equation of PGM as oxides in silicate melts,

$$M(metal) + (m/4)O_2 = MO_{m/2}(melt). \quad (1)$$

As follows from the equilibrium constant,

$$\log C(M)\ melt = (m/4) \cdot \log f_{O_2} + const. \quad (2)$$

Under high water pressure, PGM can dissolve as hydroxides according to the reaction

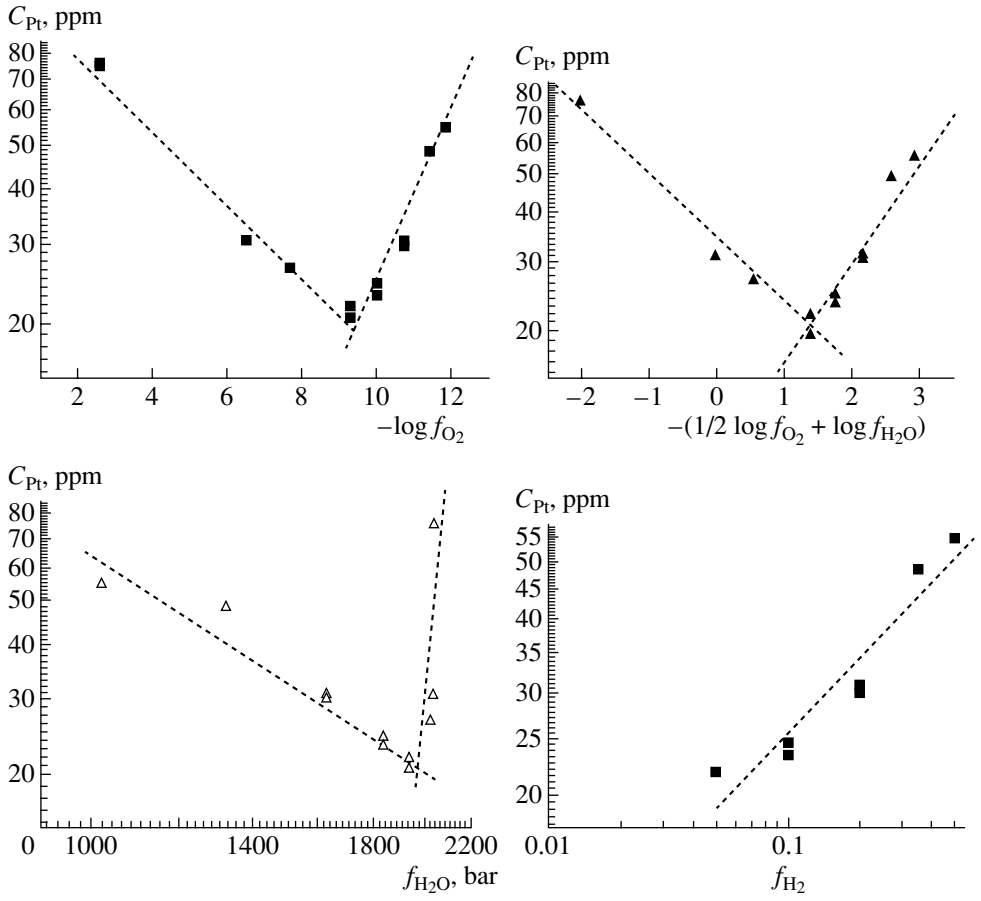

Fig. 1. Dependence of Pt solubility in the water-saturated DAA melts at 1200°C and 2 kbar on the fugacity of major fluid components (oxygen, water, and hydrogen). The Pt solubility and fugacities are shown in logarithmic scale. Dependence of C_{Pt} on hydrogen fugacity is given only for reducing conditions.

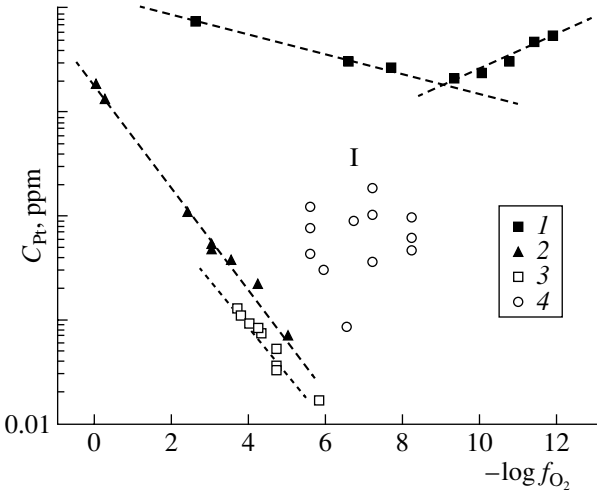

Fig. 2. Dependence of Pt solubility in the Fe-free haplobasaltic melts on f_{O_2}. (*1*) Our data, water-saturated melt, T = 1200°C, P = 2 kbar; (*2*) data after [4], T = 1400°C, P = 1 atm; (*3*) data after [2], T = 1250°C, P = 2 kbar; (*4*) data after [4], T = 1400°C, P = 1 atm; (I) Field related to the micronugget effect.

$$\mathrm{M(metal)} + (m/4)\mathrm{O_2} + (m/2)\mathrm{H_2O} = \mathrm{M(OH)}_{m/2}\mathrm{(melt)}. \quad (3)$$

As seen from Eq. (3), PGM solubility depends not only on f_{O_2}, but also on f_{H_2O}.

Equation (3) can be presented as follows:

$$\mathrm{M(metal)} + (m/2)[1/2\mathrm{O_2} + \mathrm{H_2O}] = \mathrm{M(OH)}_{m/2}\mathrm{(melt)}, \quad (4)$$

Hence,

$$\log C(\mathrm{M})\mathrm{melt} = m/2[1/2 \log f_{O_2} + \log f_{H_2O}] + \mathrm{const} \quad (5)$$

(hereinafter, m is the effective valence of PGM in a silicate melt). Equations (2) and (5) demonstrate a linear dependence between $\log C_{Pt}$ in the melt and the logarithm of the fugacities of O_2 and H_2O. The slope coefficient k is the tangent of slope of the linear dependence $\log C_{Pt} - \log f_{O_2}$ (coefficient of $\log f_{O_2}$ in the $\log C_{Pt} -$

$\log f_{O_2}$ dependence) and must be equal to m/4. Hence, the effective Pt valence in a melt is 4m. For the $\log C_{Pt} - [1/2 \log f_{O_2} + \log f_{H_2O}]$ relationship involving the influence of oxygen and water fugacity on the Pt solubility, the angle coefficient is $k = m/2$ and the effective valence is $2m$.

According to our data, the Pt dependence on f_{O_2} and f_{H_2O} in the oxidizing range is described by the equations

$$\log C\text{Pt(ppm)} = 2.093 + 0.087 \log f_{O_2}, \quad (6)$$

$$\log C\text{Pt(ppm)} = 1.522 + 0.172[1/2 \log f_{O_2} + \log f_{H_2O}]. \quad (7)$$

The angle coefficient k is 0.087 and 0.172, respectively, which corresponds to an effective Pt valence of 1/3. Thus, regardless of the form in which the reaction of Pt solubility is written (in oxide or hydroxide forms), the effective valence of Pt is similar.

The dependence of Pt solubility on f_{H_2O} is shown in Fig. 1. Under oxidizing conditions (f_{O_2} from HM to NNO), water fugacity decreases insignificantly (from 2039 to 2035), whereas f_{O_2} decreases from –2.58 to –7.67, and Pt solubility decreases from 52 to 23 ppm. Thus, assuming Pt solubility in oxide and hydroxide forms, the decrease in Pt solubility is mainly caused by changes of f_{O_2}.

However, this conclusion cannot be considered as final. At high water pressure, the observed PGM solubility reflects the total influence of the fugacities of all fluid components (oxygen, water, and hydrogen), which are related by the water dissociation equation: $H_2O = H_2 + 1/2\,O_2$ with equilibrium constant $K = f_{H_2} \cdot (f_{O_2})^{1/2}/f_{H_2O}$. The proposed formal thermodynamic models of PGM solubility in silicate melts (Eqs. (1) and (3)) do not account for variations in the contents of free (molecular) and ionic species of water in silicate melts in the case of a simultaneous decrease in f_{O_2} and increase in f_{H_2}. Since ionic water in the haplobasaltic melt is primarily bound with Na, PGMs interact with free molecular water during dissolution in hydroxide form. If the content of molecular water in the melt varies with a decrease in f_{O_2} and increase in f_{H_2}, even insignificant variations in water fugacity will affect PGM solubility.

Under reducing conditions, Pt solubility shows an inverse correlation with f_{O_2} and f_{H_2O}:

$$\log C_{Pt}\,(\text{ppm}) = 0.315 - 0.172 \log f_{O_2}, \quad (8)$$

$$\log C_{Pt}\,(\text{ppm}) = 0.902 - 0.285\,[1/2 \log f_{O_2} + \log f_{H_2O}], \quad (9)$$

where the angle coefficients $k = 0.172$ and 0.285, respectively, correspond to an effective valence of Pt ranging from 2/3 to 3/5.

Of special interest are the following two main results: (1) the higher Pt solubility in the water-saturated haplobasaltic melt as compared to that in "dry" melts at a high (2 kbar) pressure of water–hydrogen fluid; (2) the inversion of Pt solubility versus f_{O_2} dependence from a positive to negative relationship under reducing conditions (f_{O_2} < MW) (Figs. 1, 2). The comparison of Pt solubility in the water-saturated haplobasaltic melt at 2 kbar and in the "dry" melt at 1 atm showed that Pt solubility in the hydrous melts is higher ($10n$ ppm) than in the "dry" melts (<1 ppm). These differences can be explained by the influence of both f_{O_2} and f_{H_2O} on solubility, as follows from Eq. (3). Since $f_{O_2} > 1000$ at a water–hydrogen fluid pressure of 2 kbar within the entire f_{H_2O} interval, the Pt solubility in the water-bearing melt must be higher than that in the "dry" water-free melts by $\frac{m}{2} \log f_{H_2O}$. The same reason explains the slower decrease of Pt solubility in the water-bearing melt relative to "dry" melts with decreasing f_{O_2}. Correspondingly, the angle coefficient (slope of the $\log C_{Pt} - \log f_{O_2}$ curve) is also lower.

Data on Pt solubility in the water-bearing haplobasaltic melt at 1250°C and 2 kbar and f_{O_2} from –3.5 to –6 logarithmic units are presented in the recent work [2]. It was found that the Pt solubility has a positive correlation with f_{O_2}. However, unlike our experimental data, Pt solubility in [2] was comparable ($10n$ ppm) with that in "dry" melts (Fig. 2). According to [2], the increase in Pt solubility with increasing water content in the melt is related to the f_{O_2} increase, and water fluid does not affect the Pt solubility in the silicate melt.

We believe that such a disagreement is caused by a difference in experimental conditions. In our experiments, the melt was permanently affected by the water fluid pressure, and volatiles of its components were determined by the mole fraction of introduced hydrogen. This provided constant concentrations and proportions between molecular and dissociated waters in the melt in each experiment. As is known, water in silicate melts dissolves in the molecular and dissociated forms. The dissociated (bound) water forms steady compounds with alkali and alkali earth elements. The molecular (unbound) water can form hydrate complexes with metals in the melt and can easily exsolve from the melt in an undersaturated environment. In the autoclave experiments [2], silicate sample with a small amount of water (insufficient to saturate the melt at

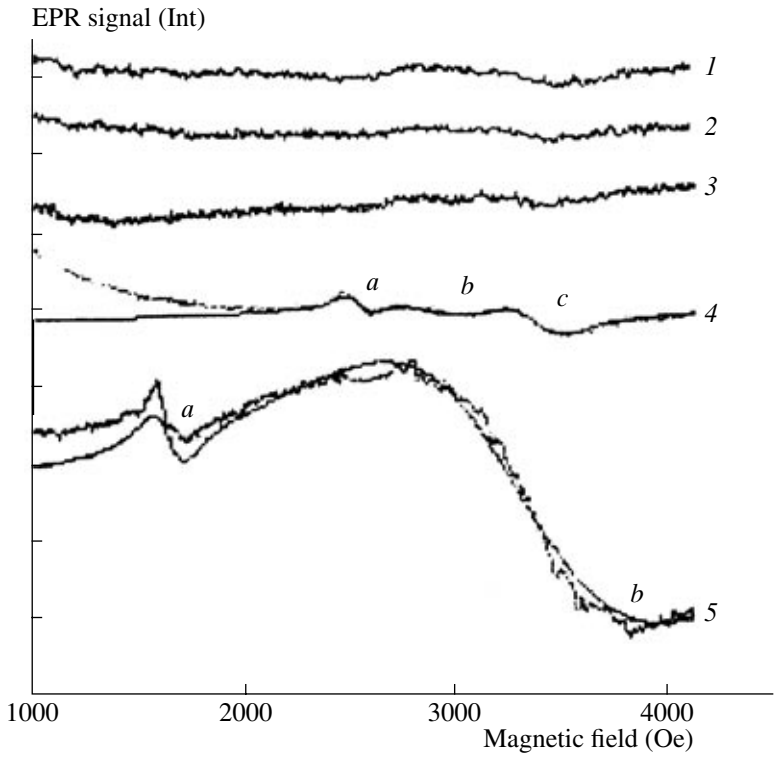

Fig. 3. EPR spectra (*1–4*) of the water-bearing glass from experiments on Pt solubility in the water-saturated DAA melts at 1200°C and 2 kbar at different f_{O_2} values (in lg units): (*1*) $\log f_{O_2} = -2.58$ (HM); (*2*) –7.67 (NNO); (*3*) –9.3 ($x_{H_2} = 0.05$); (4) –11.39 ($x_{H_2} = 0.35$); (*5*) EPR spectrum of the control sample of silicate glass with microinclusions of metallic Pt. No EPR signal is observed in spectra *1–3*. Spectrum *4* demonstrates a weak EPR signal with three signals (*a, b, c*) in the EPR spectrum. Spectrum *5* exhibits two distinct EPR signals (*a, b*), which do not coincide with those in spectrum 4.

given *T* and *P*) was placed in the Pt ampule. The low starting water content in the system and its decomposition owing to continuous H_2 loss from the Pt ampule must lead to the steady oversaturation of the melt and to the consequent exsolution and removal of molecular water from the melt. Owing to the loss of molecular water in the experiments [2], melts (and quenched glasses) contained only bound water, which showed no effect on the Pt solubility.

Let us consider the contamination by microscopic inclusions of metals (i.e., the "nuggets" problem). The nature and formation mechanisms of the microinclusions are still unclear. According to [4, 7, 8], metallic inclusions form at a low oxygen fugacity. In the $\log C_{Pt} - \log f_{O_2}$ diagrams, $\log C_{Pt}$ shows a linear dependence on $\log f_{O_2}$ with decreasing f_{O_2}, beginning from atmospheric oxidizing conditions. At lower f_{O_2} values ($f_{O_2} \le$ NNO), the linear dependence is disturbed and one can see a chaotic distribution of experimental points above the $\log C_{Pt} - \log f_{O_2}$ trend (nuggets effect, Fig. 3). The replacement of the linear dependence by chaotic distribution can serve as evidence for glass contamination by microinclusions of metallic Pt (if the observed nuggets effect is actually related to the formation of metallic microinclusions). In our experiments, the positive linear correlation $\log C_{Pt} - \log f_{O_2}$ was observed within a significantly wider f_{O_2} interval (from MH to IW buffers). In addition, experimental glasses were analyzed by the electron paramagnetic resonance (EPR) method to determine the modes of Pt occurrence.

The latter is a sensitive method for the investigation of modes of metal occurrence in glasses, beginning from a sensitivity of paramagnetic ion of 10^{11} spin/Oe, which corresponds to PGM contents of 1–100 ppm. The EPR spectra of experimental samples were compared to that of the control sample with microinclusions of metallic Pt (Fig. 3). The control sample was synthesized by melting powdered Pt 5–10 μm in size (black Pt) and haplobasaltic glass at 1300°C for 10 min. No EPR signal was recorded from glasses obtained at a temperature of *T* = 1200°C, water fluid pressure of 2 kbar, and $\log f_{O_2}$ from –2.6 (MH buffer) to – 9.3 ($XH_2 = 0.05$) (curves *1–3*). A weak EPR signal (curve *4*) was observed at $\log f_{O_2} = -11.4$ ($XH_2 = 0.35$). The EPR signal of the control sample (spectrum 5) contained two lines, which differed from those in the spec-

trum of the experimental sample obtained under reducing conditions (spectrum *4*). The absence of paramagnetic ion in silicate glasses (spectra *1–4*) indicates the absence of the contamination of the melt by microparticles of the metallic phase. Hence, the high Pt solubility in our experiments is not related to the contamination by metallic Pt from ampule.

The second main result is the inversion of dependence of Pt solubility on f_{O_2} from positive to negative under reducing conditions (f_{O_2} < MW buffer). Owing to the microinclusion problems, the Pt solubility versus f_{O_2} relationship showed no inversion in some experimental works in the water-free silicate melts at 1 atm. The opposite dependence of Pt solubility on f_{O_2} within $\log f_{O_2}$ from –4 to –7 was observed in [3], while a similar inversion in the Pt solubility depending on f_{O_2} was observed in [7]. The cause of this inversion is not exactly clear. Some authors suggest its relation with the presence of zero-valent Pt in the melt with the simultaneous passivation of metal and the formation of oxide film on its surface according to the reaction Pt (melt) + O_2 = PtO_2 (metal surface) [9]. Others [4, 8] assume that Pt interacts with silica acid or microimpurities of the melt to form the low-temperature eutectics. In the case of convection, silicate melt is "polluted" by microinclusions of eutectic PGM melt.

An interesting idea was proposed in [9]. It assumes that the increase of Pt solubility with f_{O_2} decrease under reducing conditions is related to the presence of the negatively-charged Pt in the melt. In this case, the Pt solubility can be expressed by the equation

$$\mathrm{Pt(metal)} + \frac{m}{2}\mathrm{H_2} = \mathrm{PtH}_m\mathrm{(melt)}, \qquad (10)$$

the equilibrium constant of which shows that $\log C_{Pt} = k \log f_{H_2}$ + constant, where $k = \frac{m}{2}$, $m = 2k$.

Figure 1 demonstrates the dependence of Pt solubility on f_{H_2} for reducing conditions, which is described by the equation

$$\log C_{Pt} = 0.528 + 0.364 \log f_{H_2}. \qquad (11)$$

This equation shows that the negative effective valence of Pt is 0.72. It is interesting that, regardless of the thermodynamic model of dissolution, the effective valence of Pt under reducing conditions, as calculated from experimental data on $\log C_{Pt} - \log f_{O_2}$, $\log C_{Pt} - \log\left[\frac{1}{2}\log f_{O_2} + \log f_{H_2O}\right]$, and $\log C_{Pt} - \log f_{H_2}$ relationships, have a similar effective valence. However, two former relationships deduced from the solubility of Pt as positively charged oxides or hydroxides (Eqs. (1) and (3)) require a positive dependence of solubility on f_{O_2} and f_{H_2O}, which is inconsistent with experimental data. The thermodynamic model of Pt solubility in the negatively charged form, as hydride according to Eq. (10), agrees with experimental data. Hence, the assumption of Pt solubility in a negatively charged form under reducing conditions seems to be a realistic one.

ACKNOWLEDGMENTS

This work was supported by the Russian Foundation for Basic Research (project nos. 03-05-64535 and 03-05-64549) and the Division of Earth Sciences of the Russian Academy of Sciences (Program no. 9-5).

REFERENCES

1. W. Ertel, M. Pichvant, B. Scaillet, *et al.*, Miner. Mag. **62a**, 425 (1998).
2. F. A. Blaine, R. L. Linnen, F. Holtz, *et al.*, Geochim. Cosmochim. Acta **69**, 1265 (2005).
3. J. Amosse, M. Allibert, W. Fischer, *et al.*, Chem. Geol. **81**, 45 (1990).
4. A. Borisov and H. Palme, Geochim. Cosmochim. Acta **61**, 4349 (1997).
5. N. I. Bezmen, Petrologiya **9**, 398 (2001) [Petrology **9**, 345 (2001)].
6. E. Azif, M. Pichvant, and T. Auge, Terra Nova, Suppl. 1, 1 (1994).
7. W. Ertel, H. St. C. O'Neil, P. J. Sylvester, *et al.*, Geochim. Cosmochim. Acta **63**, 2439 (1999).
8. A. Borisov and H. Palme, Am. Mineral. **85**, 1665 (2000).
9. J. Amosse, P. Dable, and M. Allibert, Mineral. Petrol. **68**, 29 (2000).